SURFACE TREATMENT OF POLYPROPYLENE USING A CAPACITIVELY COUPLED PLASMA SYSTEM

A THESIS SUBMITTED TO
THE GRADUATE SCHOOL OF NATURAL AND APPLIED SCIENCES
OF
MIDDLE EAST TECHNICAL UNIVERSITY

BY

GİRAY MECİT

IN PARTIAL FULFILLMENT OF THE REQUIREMENTS
FOR
THE DEGREE OF MASTER OF SCIENCE
IN
PHYSICS

FEBRUARY 2022

Approval of the thesis:

SURFACE TREATMENT OF POLYPROPYLENE USING A CAPACITIVELY COUPLED PLASMA SYSTEM

submitted by **GİRAY MECİT** in partial fulfillment of the requirements for the degree of **Master of Science in Physics Department, Middle East Technical University** by,

Prof. Dr. Halil Kalıpçılar
Dean, Graduate School of **Natural and Applied Sciences** _____

Prof. Dr. Seçkin Kürkcüoğlu
Head of Department, **Physics** _____

Assoc. Prof. Dr. Burak Yedierler
Supervisor, **Physics, METU** _____

Examining Committee Members:

Assoc. Prof. Dr. Kemal Efe Eseller
Electrical and Electronical Engineering, Atılım University _____

Assoc. Prof. Dr. Burak Yedierler
Physics, METU _____

Prof. Dr. İsmail Rafatov
Physics, METU _____

Date: 11.02.2022

I hereby declare that all information in this document has been obtained and presented in accordance with academic rules and ethical conduct. I also declare that, as required by these rules and conduct, I have fully cited and referenced all material and results that are not original to this work.

Name, Surname: Giray Mecit

Signature :

ABSTRACT

SURFACE TREATMENT OF POLYPROPYLENE USING A CAPACITIVELY COUPLED PLASMA SYSTEM

Mecit, Giray
M.S., Department of Physics
Supervisor: Assoc. Prof. Dr. Burak Yedierler

February 2022, 35 pages

Gaseous plasmas are suitable for various applications in material science, including but not limited to thin film productions and coatings, tailoring the surface properties of polymers. This study aims to characterize a capacitively coupled plasma system utilized in material processing applications. The system utilizes a 13.56 MHz radio frequency source to produce gaseous plasmas. The correlation between the produced plasmas and the surface physical and surface chemical properties of polypropylene treated by such plasmas are in the interest of many novel research applications. The treatments are done using Argon and Nitrogen plasmas separately, while the flow rates of all gasses are controlled using a multi-gas controller. Investigations of changes on PP surface are done employing FTIR-ATR, XRD, SEM analyses. Results of this study, the crystallinity of PP surface is improved, and newly formed chemical and physical structures are observed.

Keywords: plasma treatment, polypropylene, plasma surface modification

ÖZ

POLİPROPİLEN YÜZEYİNİN SIĞAL BAĞLAŞIMLI PLAZMA SİSTEMİ KULLANILARAK İŞLENMESİ

Mecit, Giray
Yüksek Lisans, Fizik Bölümü
Tez Yöneticisi: Doç. Dr. Burak Yedierler

Şubat 2022 , 35 sayfa

Gaz içerikli plazmalar malzeme biliminin ince film üretimi ve kaplamaları, polimerlerin yüzey özelliklerinin iyileştirilmesi gibi çeşitli aplikasyonları için uygundur. Bu çalışma, bu tip malzeme işleme uygulamalarında kullanılan bir sığal bağlaşımlı plazma sistemini karakterize etmeyi amaçlamaktadır. Gazlı plazma üretmek için 13.56 MHz radyo frekans kaynağı kullanılır. Oluşturulan plazma ve bu plazma ile plazma ile işlenen polipropilenin yüzey fiziksel ve yüzey kimyasal özellikleri arasındaki korelasyon, birçok yeni araştırma uygulamasının ilgisini çekmektedir. İşlemeler Argon ve Azot plazmalarını ayrı kullanarak oluşturulur, tüm gazların akış hızları bir çoklu gaz kontrolcüsü kullanılarak kontrol edilir. PP yüzeyindeki değişikliklerin incelemeleri FTIR-ATR, XRD, SEM tanı metotları kullanılarak yapılır. Bu çalışmanın sonucunda, PP yüzeyinin kristalliğinin iyileştirildi ve yeni oluşan kimyasal ve fiziksel yapılar gözlendi.

Anahtar Kelimeler: plazma işlem, polipropilen, plazma yüzey modifikasyon

to painkillers

ACKNOWLEDGMENTS

I would like to express my deepest appreciation to my current and former advisors for their unwavering guidance.

I would like to extend my sincere thanks to the lab members and my friends for their profound belief in my work and to "recover" me after COVID related mental breakdown.

I would also like to extend my deepest gratitude to my committee for their helpful advice.

Part of this work is supported by the Scientific Research Project Fund of Middle East Technical University BAP-01-05-2017-006 and BAP-08-11-2017-040

TABLE OF CONTENTS

LIST OF TABLES

TABLES

LIST OF FIGURES

FIGURES

LIST OF ABBREVIATIONS

PP	Polypropylene
IRE	Internal Reflection Element
ATR	Attenuated Total Reflection
XRD	X-Ray Diffraction
SEM	Scanning Electron Microscopy
sccm	Standard Cubic Centimeter per Minute

CHAPTER 1

INTRODUCTION

Plasma discharge is frequently used to improve the surface characteristics of polymers, such as adhesion, wettability, printability, and biocompatibility[1, 2]. Polypropylene (PP) is one of the most produced synthetic plastic given that it has excellent properties such as good chemical resistivity, transparency, high thermal resistance, and it is a low-cost material. Due to its low surface free energy, PP is usually not suitable for some industrial or medical applications that require good surface characteristics[3]. Adhesion is the tendency of different particles to cling to one another. The wetting phenomenon explains how liquids move when dropped to a given solid surface. On a glass surface, for example, a water drop spreads out. It does not, however, spread out on a plastic surface. Printability describes how printable the material's surface is, which is very important for industrial applications to improve print quality. Biocompatibility is how the material is compatible with living tissue. Many chemical and physical techniques have been used to improve the surface characteristics of polymers. Plasma surface modification is one of the physical techniques that has been commonly used to change and improve surface characteristics[4]. This technique is considered more advantageous due to its environmentally friendly process, and it only acts the upper layer of the surface around a few nanometers without changing the bulk properties of the material. Unlike other techniques, this does not require any additional material or solution. Due to these reasons, plasma surface modifications are considered among the most commonly studied research topics, yet there is much to discover.

1.1 Plasma Physics

A plasma, in general, is an ionized gas composed of charged particles that are nearly neutral. Heating an ordinary gas produces plasmas if the random kinetic energy of gas molecules is sufficient to break molecular bonds. That is, the kinetic energy exceeds ionization energy. When gas molecules collide with another one, some of the electrons might be released from the atoms. Thus, there would be free electrons, ions and neutral gas molecules. This could be done by employing photons to interact with an ordinary gas rather than heating the gas. The light source must be sufficient to sustain a high ionization rate to keep plasmas up [5].

Unlike common sense, plasmas would not be the fourth state matter. This is because the universe mainly consists of hot objects in the plasma state. Naturally, gasses are obtained by cooling plasmas. In this sense, plasma is the first state of matter. However, it is impossible to utilize naturally occurring plasmas for any practical purpose [6]. Plasmas could roughly be classified into two groups: natural and man-made ones. Many natural plasmas can be observed with ease as they radiate electromagnetic waves. Irving Langmuir's gas discharges kicked off plasma research almost a hundred years ago[7]. Since plasmas consist of charged particles, macroscopic forms of Maxwell's equations are valid for plasmas.

$$\begin{aligned}
\vec{\boldsymbol{\nabla}} \times \vec{E}(\vec{r},t) &= -\mu_0 \frac{\partial}{\partial t}\vec{H}(\vec{r},t) \\
\vec{\boldsymbol{\nabla}} \times \vec{H}(\vec{r},t) &= \vec{J}(\vec{r},t) + \epsilon_0 \frac{\partial}{\partial t}\vec{H}(\vec{r},t) \\
\epsilon_0 \vec{\boldsymbol{\nabla}} \cdot \vec{E}(\vec{r},t) &= \rho(\vec{r},t) \\
\mu_0 \vec{\boldsymbol{\nabla}} \cdot \vec{H}(\vec{r},t) &= 0
\end{aligned} \tag{1.1}$$

where $\vec{E}(\vec{r},t)$ and $\vec{H}(\vec{r},t)$ are electric and magnetic field vectors, and where ϵ_0 and mu_0 are the permittivity and permeability of free space. The source terms $\vec{J}(\vec{r},t)$ and $\rho(\vec{r},t)$ are the electrical current and charge densities, and these two densities are related by a charge continuity equation:

$$\frac{\partial}{\partial t}\rho(\vec{r},t) + \vec{\boldsymbol{\nabla}} \cdot \vec{J}(\vec{r},t) = 0 \tag{1.2}$$

In a plasma in vacuum, $\vec{J}(\vec{r},t) = \vec{J}_c(\vec{r},t)$ and it is the conduction current density. There are no effects of magnetization and polarization current densities on these type

of plasmas. Also, the magnetic field does not much change in time in plasmas[8]. Thus, the electric field is an irrotational vector field.

$$\vec{\nabla} \times \vec{E}(\vec{r}, t) = 0 \tag{1.3}$$

One can utilize this property to find the electric potential, $\Phi(\vec{r}, t)$.

$$\vec{E}(\vec{r}, t) = -\vec{\nabla}\Phi(\vec{r}, t) \tag{1.4}$$

Since plasmas could be considered as fluids, fluid dynamics equations are taken into account. For any particle, its kinetic energy, E, is calculated using a simple relation

$$E = \frac{1}{2} m \vec{v}^2 \tag{1.5}$$

where m is the mass of the particle and $\vec{v}$ is the velocity of the particle. Since there are many particles, an average value for the kinetic energy is more meaningful. The average kinetic for N-particle system, E_{av}, is given as:

$$E_{av} = \frac{1}{2N} \sum_{n=1}^{N} m_i \vec{v}_i^2 \tag{1.6}$$

Then, the average kinetic energy of ordinary gasses in thermal equilibrium, E, is defined as:

$$E = \frac{3}{2} k_B T \tag{1.7}$$

where k_B is Boltzmann's constant and T is gas temperature. Ordinary gasses in thermal equilibrium obey Maxwellian velocity distribution function, and 1-D version of Maxwellian velocity distribution function is given as:

$$f(v) = A e^{-\frac{mv^2}{2k_B T}} \tag{1.8}$$

where $A = N\sqrt{\frac{m}{2\pi k_B T}}$. Two different averaging methods are available for the velocity, namely linearly averaged velocity, $\bar{v}$ and root-mean-square(rms) velocity, $\overline{v_{rms}}$.

$$\begin{aligned} \bar{v} &= \int v f(v) \mathrm{d}v \\ \overline{v_{rms}} &= \sqrt{\left| \int v^2 f(v) \mathrm{d}v \right|} \end{aligned} \tag{1.9}$$

By computing these integrals, $\bar{v}$ and $\overline{v_{rms}}$ are found as $\sqrt{\frac{8k_B T}{\pi m}}$ and $\sqrt{\frac{3k_B T}{m}}$, respectively. One the one hand, these equations are valid for single fluid. On the other hand,

the plasma consists of electrons, ions and unionized gas molecules. It is also possible to have more than one type of ion in plasmas. Due to the quasi-neutrality of plasmas, there should be almost equal amount of positive and negative charges.

$$n_e \approx \sum_j n_{ij} \approx n \tag{1.10}$$

where n_e, n_i and n are the number density of electrons, ions and the plasma, respectively, and j refers to different types of ions.

The temperature of electrons, T_e, ions T_i and gas molecules, T_g could be defined, and these temperature values would be different because of different kinetic energies. By comparing temperatures, plasma can be categorized in two groups: cold plasmas and hot plasmas [9]. In this study, weakly ionized cold plasmas in the absence of a magnetic field are employed. In cold plasmas, $T_e > T_i \approx T_g$. That is, electrons are more energetic than ions and gas molecules. Electrons and ions are accelerated by the Lorentz force, $\vec{F}_L$.

$$\vec{F}_L = q\vec{E} \tag{1.11}$$

where q is the charge of the plasma species. Electrons collide with ions and gas molecules as they gain energy from the electric field in the plasma. If there is no change in internal energy, these collisions are called elastic collisions. If the internal energy is exchanged between plasma species, these collisions are called inelastic collisions. The gas molecules are excited and ionized as a result of these collisions. In cold plasmas, ionization sustains the plasma. The ratio of transferred, E_t, and initial, E_i, kinetic energies is given as:

$$\frac{E_t}{E_i} = \frac{4m_1m_2\cos^2\theta}{(m_1+m_2)^2} \tag{1.12}$$

where m_1, m_2 are the masses of particles, and θ is the collision angle[8].

To further understand the basics of plasma physics, the velocity distribution function of electrons in the velocity space is employed.

$$n(\vec{x},t) = \int f(\vec{v},\vec{x},t)\mathrm{d}\vec{v} \tag{1.13}$$

Where $n(\vec{x},t)$ is number density and $\mathrm{d}\vec{v} = \mathrm{d}v_x\,\mathrm{d}v_y\,\mathrm{d}v_z$ that is the volume element in the velocity space. For unmagnetized plasmas, the Boltzmann equation with collision terms is given as:

$$\frac{\partial}{\partial t}f + \vec{v}\cdot\vec{\boldsymbol{\nabla}}_{\vec{x}}f - \frac{q_e}{m_e}\vec{E}\cdot\vec{\boldsymbol{\nabla}}_{\vec{v}}f = C^{el}(f) + \sum_l C_l^{ie}(f) \tag{1.14}$$

where q_e and m_e are the charge and mass of the electron, and $C^{el}(f)$ and $C_l^{ie}(f)$ denote collision terms for elastic and inelastic collisions, respectively [10]. To find collision terms, moments of the Boltzmann are taken. To find a moment of the Boltzmann equation for an arbitrary function, $\Omega(\vec{v}, \vec{x}, t)$, following calculation is done.

$$\int \Omega[\frac{\partial}{\partial t} f + \vec{v} \cdot \vec{\nabla}_{\vec{x}} f - \frac{q_e}{m_e} \vec{E} \cdot \vec{\nabla}_{\vec{v}} f] \mathrm{d}\vec{v} = \int \Omega[C^{el}(f) + \sum_l C_l^{ie}(f)] \mathrm{d}\vec{v} \quad (1.15)$$

These integrals are over all velocities. $\Omega(\vec{v}, \vec{x}, t)$ could be 1, $m_e\vec{v}$ or $\frac{1}{2}m_e|\vec{v}|^2$, and corresponding moments are known as 0^{th}, 1^{st}, 2^{nd} moments of the Boltzmann equation.

1.2 Polypropylene

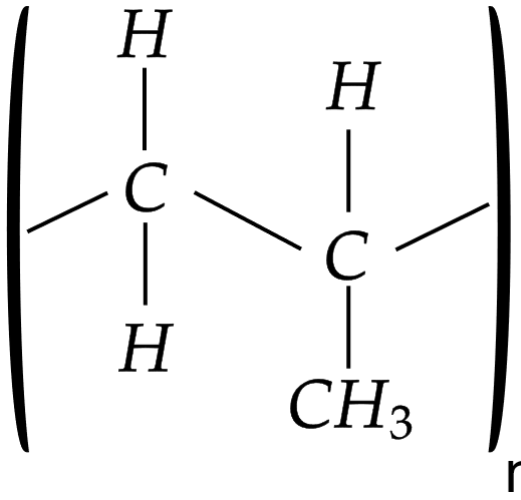

Figure 1.1: Molecular structure of Polypropylene

Polypropylene (PP) is one of the most produced synthetic plastics. It has excellent properties such as good chemical resistivity, transparency, high thermal resistance, and it is cheaper than most of the materials. These properties make it one of the best choices for applications that do not require regular maintenance, such as implants because there is no corrosion and a long degradation time. Due to its low surface energy, PP is needed to be improved for industrial or medical applications requiring good surface characteristics. Many chemical and physical techniques have been used to improve the surface characteristics of polymers such as plasma-enhanced chemical

vapor deposition, impulse corona discharge, surfactant immobilization and air dielectric barrier discharge. Plasma surface treatment is one of the physical techniques that has been commonly used to change and enhance surface characteristics[11, 12].

CHAPTER 2

THE EXPERIMENT

In this section, the sample preparation process, the treatment system and treatment parameters are discussed.

2.1 Sample Preparation

PP beads were produced by PETKIM with more than 90% purity, as shown in Figure 2.1. They were cleaned using laboratory-grade acetone, isopropyl alcohol and ethanol, and were dried in ambient conditions. They were melted at 160 °C and

Figure 2.1: PP beads

pressed using a hot press (Rucker PHI). A rectangular sheet of PP was made at 140 PSI and 200 °C. The sheet had approximately 220 cm^2 area with a thickness of 0.6 cm. It was cut into smaller pieces with an area of approximately 1.5 cm^2, as shown in Figure 2.2. These smaller pieces of PP were employed during the plasma treatment.

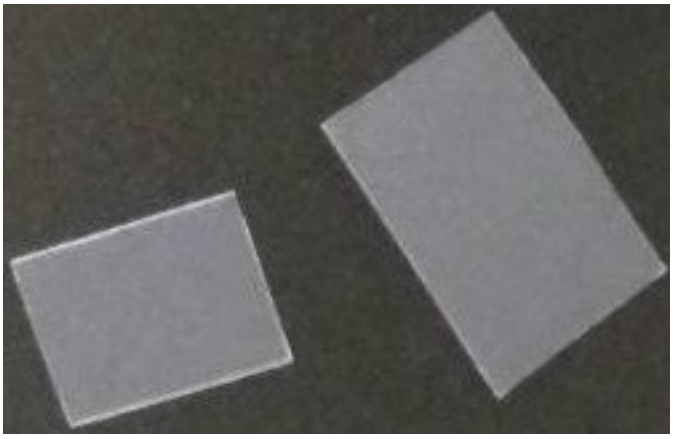

Figure 2.2: PP samples

2.2 Experimental Setup

Capacitively coupled plasma system with a 13.56 MHz RF source (Cesar®, Advanced Energy Industries, Inc.) and a dual-stage rotary vane pump (Varian DS-302) treated PP samples. The setup is shown in Figure 2.3. The aluminium electrodes have a

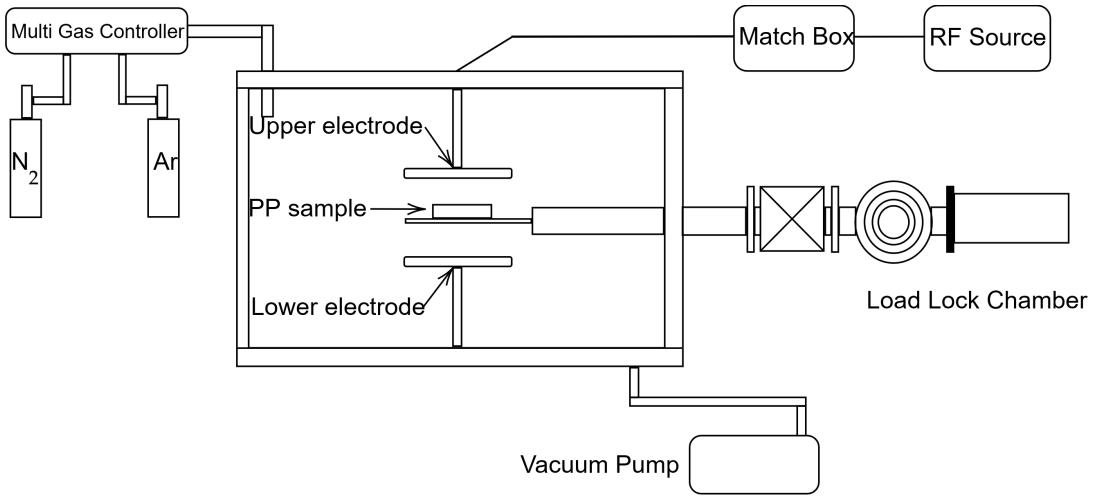

Figure 2.3: Capacitively coupled RF plasma system

cylindrical geometry. The upper one was connected to the RF source, whereas the lower one was grounded. Thanks to MKS™ multi-gas controller 647C, the gas flow rate was constant at 50 standard cubic centimeters per minute(sccm). Only one type of gas was introduced to the system during the treatments. In other words, the system did not contain any mixture of Ar and N_2 molecules.

2.3 Treatment of Polypropylene

The gas type and RF power were the parameters, as shown in Table 2.1.

Table 2.1: Treatment parameters

#	Gas	RF Power (W)	#	Gas	RF Power (W)
1	Ar	50	11	N_2	50
2	Ar	100	12	N_2	100
3	Ar	150	13	N_2	150
4	Ar	200	14	N_2	200
5	Ar	250	15	N_2	250
6	Ar	300	16	N_2	300
7	Ar	350	17	N_2	350
8	Ar	400	18	N_2	400
9	Ar	450	19	N_2	450
10	Ar	500	20	N_2	500

Other parameters were fixed and given as below.

- Treatment pressure is 1.2×10^{-1} torr.
- Treatment duration is 10 minutes.
- Gas flow rate is 50 sccm.

Twenty pieces of PP samples were treated. All samples were placed at the exact position of the plasma chamber. These parameters were chosen in light of my previous studies in POLAR Laboratories at METU.

CHAPTER 3

INSTRUMENTATION

3.1 Attenuated Total Reflection-Fourier Transform Infrared Spectroscopy

Attenuated total reflection (ATR) is one of several techniques in infrared spectroscopy. This technique has significant advantages, such as no sample preparation is needed, and the sample is not affected. In this technique, the sample is in contact with the sensing element, and a spectrum is received due to this contact. A beam of infrared light is transmitted through the sensing element; therefore, there is no thickness limitation on the sample size to transmit the incident beam. Sample morphology can be anything if there is a sufficient contact area.

When light travels from a medium to another one, the angle of reflected light is governed by Snell's law.

$$n_1 \sin\theta_1 = n_2 \sin\theta_2 \tag{3.1}$$

where n_1 and n_2 are the index of refraction of medium 1 and medium 2, and θ_1 and θ_2 are the angle of incidence and refraction, respectively. n_1 is the optically dense medium if $n_1 > n_2$ and hence $\theta_1 < \theta_2$.

As the angle of incidence is increased, the refracted beam approaches $\frac{\pi}{2}$ to the normal. However, when the incident angle is equal or greater than a certain angle θ_c, the beam is reflected from the interface internally. The special angle is known as the critical angle, θ_c, and it is found as below.

$$\theta_c = \arcsin\frac{n_2}{n_1} \tag{3.2}$$

The beam travels from a high refractive index medium to a low refractive index medium, $n_1 > n_2$. These angles are measured from the surface normal to the beam. The reflectance of internal reflection equals to 1 if there is no absorption in the low

refractive index medium and those materials are called internal reflection elements (IRE). The sensing element must be an IRE. Despite the beam motion being restricted by an IRE, the light(photon) has an electromagnetic field whose direction is perpendicular to its motion.

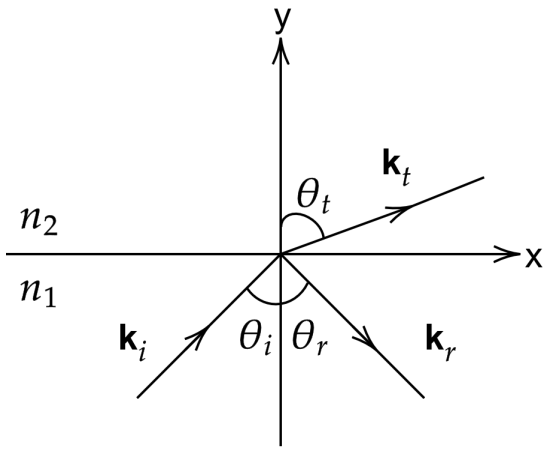

Figure 3.1: Wave vectors of the incident, reflected and transmitted fields

When the photon reaches the interference of two media, there will be a decaying electric field through less index of reflection medium and the field strength, $\mathbf{E}$, can be expressed as

$$\mathbf{E} = \mathbf{E}_0 e^{-\gamma z} \tag{3.3}$$

where $\mathbf{E}_0$ is field strength at the surface, z is the distance from the surface, and γ is a constant. This field is also known as the *evanescent wave*. Evanescent field intensity decreases to $1/e$ of surface intensity and that distance from the surface is called the *depth of penetration*, d_p and it is equal to $1/\gamma$ in Eq. 3.3. To find d_p, incident, reflected, and transmitted electric fields are considered, as shown in Figure 3.1. Despite there is no transmitted electric field and the angle with respect to the surface normal θ_t does not exist, the transmitted wave can be interpreted by allowing $\cos\theta_t$ to be complex.

$$d_p = \frac{\lambda}{2\pi\sqrt{{n_1}^2 \sin^2\theta - {n_2}^2}} \tag{3.4}$$

where λ is the free space wavelength of the incident photon, n_1 is the refractive index of the internal reflection element, n_2 is the refractive index of the sample, and θ is the angle of incidence[13].

The depth of penetration can easily be controlled by the angle of incidence and the re-

fractive index of the internal reflection element. Therefore, the examination distance would be changed with ease.
Thermo Scientific™ Nicolet™ iS™10 FTIR-ATR spectrometer was utilized, as shown in Figure 3.2

Figure 3.2: ATR measurement device with a PP sample

3.2 X-Ray Diffraction

Crystals are highly ordered regular structures. Studying the crystals' repeating part, known as a unit cell, allows us to get helpful information about the material. However, knowing a unit cell structure is not enough. How unit cells are arranged is also essential. Polymers have repeating structures, called polymer chains, but not regular as crystals. X-ray diffraction (XRD) is used to determine the properties of the crystal

structure of the sample. A coherent, monochromatic source with a wavelength comparable to the unit cell is employed. Crystals consist of equally spaced planes which are also known as Bragg planes [14]. When X-rays are sent through the material's surface at a constant angle, it is not always reflected from the same plane, as shown in Figure 3.3.

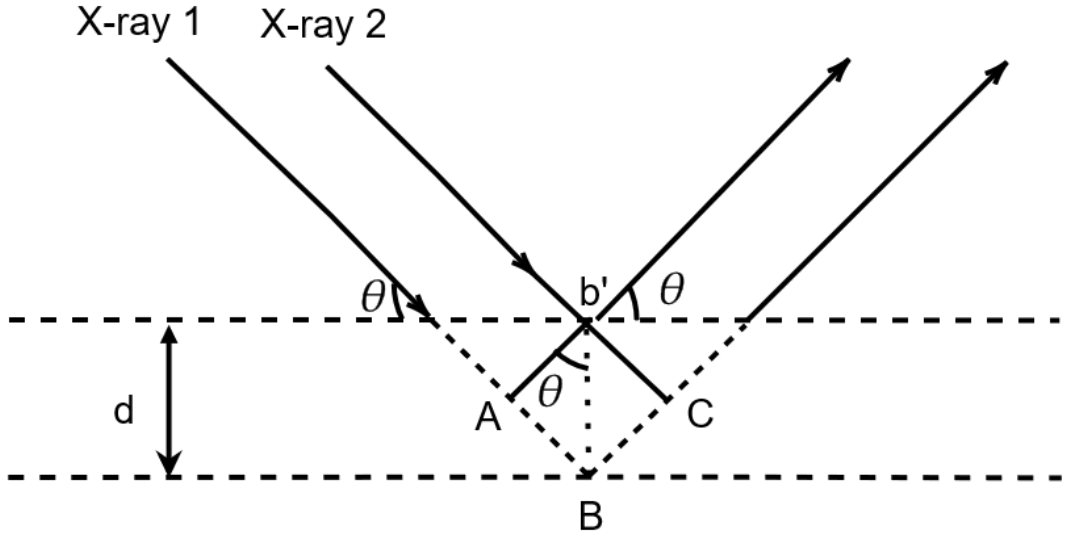

Figure 3.3: Bragg's Law

The following could be obtained using constructive interference conditions with a geometric approach. The optical path difference of the rays reflected from two consecutive planes is equal to $|AB| + |BC|$.

$$\begin{aligned} n\lambda &= |AB| + |BC| \\ |AB| &= |BC| \\ |AB| &= d\sin\theta \\ n\lambda &= 2d\sin\theta \\ \lambda &= 2d_{hkl}\sin\theta_{hkl} \end{aligned} \tag{3.5}$$

where n is the order of reflection, λ is the wavelength of X-rays, hkl are plane indices, d is the interplanar distance between two successive planes and θ is the angle of incidence. Reflected beam intensity and the angle between reflected and transmitted beams, shown as 2θ in Figure 3.4 are measured. Thus, beam intensity versus the angle data are obtained using a Rigaku Miniflex X-ray diffractometer (CuK$_\alpha$, $\lambda = 1.54$Å)

.

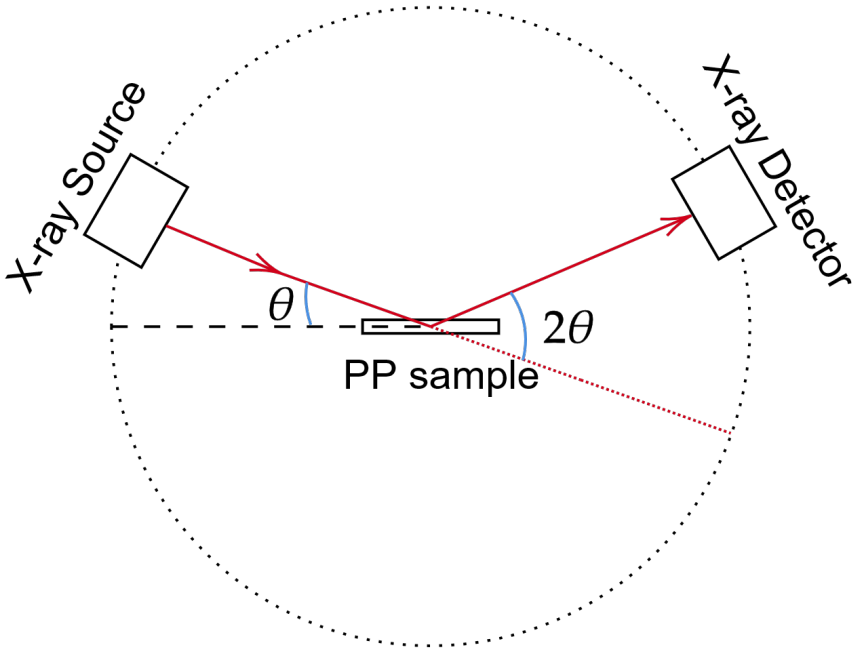

Figure 3.4: XRD measurement illustration

The crystallite size, L, can be calculated using the Scherrer equation, given as:

$$L = \frac{K\lambda}{\beta(2\theta)\cos\theta} \tag{3.6}$$

where K is the Scherrer constant, λ is the wavelength of X-rays, θ is the angle shown in Figure 3.3 and 3.4, and $\beta(2\theta)$ is the full width at half maximum[15].

3.3 Scanning Electron Microscopy

Conventional microscopes use visible light and optical lenses. In theory, the wavelength is the limiting parameter of the image's resolution. If electrons are employed as in Scanning Electron Microscopy (SEM), the resolution increases because the wavelength of electrons is much smaller than visible light. Electrons are produced and sent through a set of tools, as shown in Figure 3.5. This system, excluding the computer, the amplifier and the scan generator, is in a vacuum to eliminate interactions between electrons and the air. Electrons coming from the source hit the sample's surface and knock out electrons. Those electrons are detected by the detector connected to the

amplifier, and the back-scattered electron detector records back-scattered ones. Back-scattered electron data give low-resolution images since they collide almost elastically with the sample surface. Thus, the energy of electrons does not change much. On the other hand, electrons taken from the sample contains more detailed information. Not only they have lower energies, but also they come from within a few atomic layers of the sample [16]. The problem is that taking an electron out from the PP surface is very hard and almost impossible to do uniformly. Due to this, there is a lack of secondary electron emission, so imaging quality decreases. Although the surface coating is semi-destructive, the samples are coated with gold to make the materials' surface conduct electrons. Thus, the secondary electrons contribute to the imaging, improving the quality.

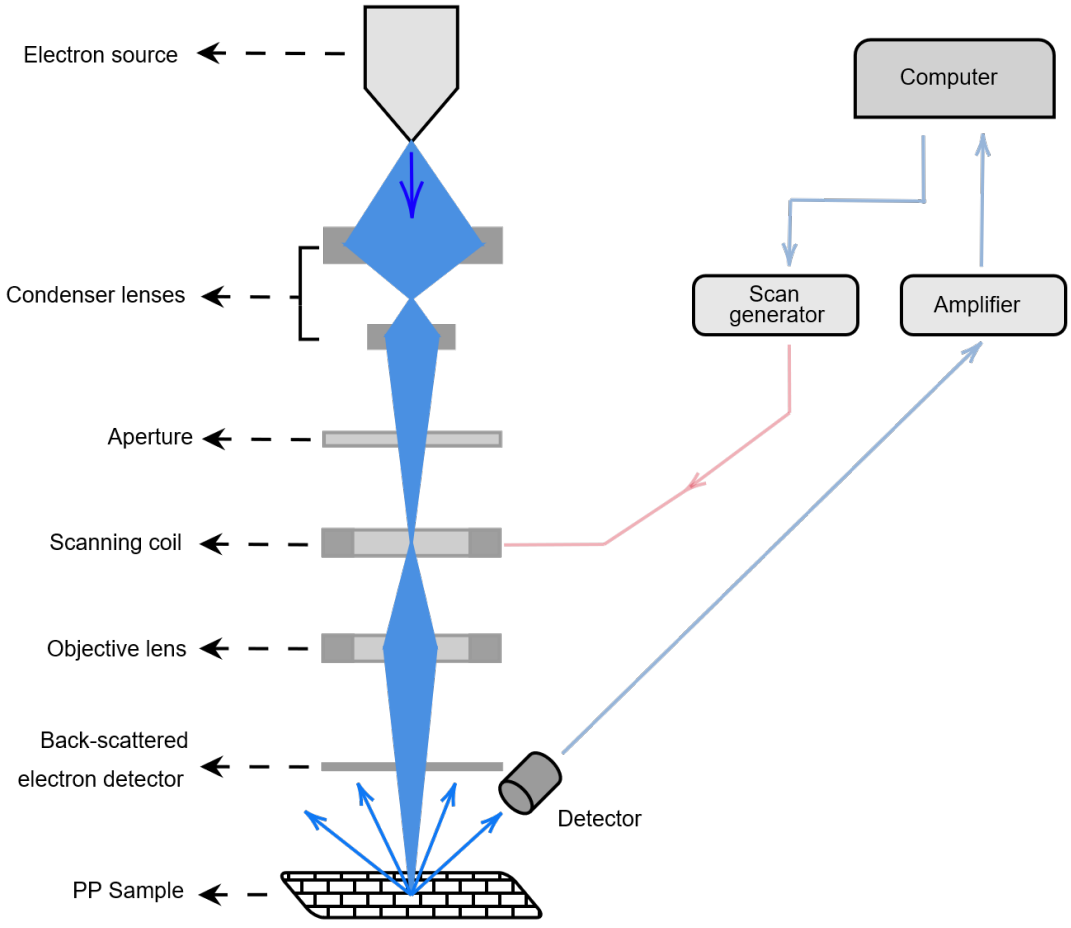

Figure 3.5: Sketch of an SEM device

The surface morphology of PP samples is examined using a QUANTA 400F Field

Emission SEM with 1.2 nm resolution.

CHAPTER 4

ANALYSIS & RESULTS

In this section, measurement range, measurement analysis and results are discussed.

4.1 Attenuated Total Reflection-Fourier Transform Infrared Spectroscopy

The aim of these measurements is to observe the change in chemical structures on the material's surface. Absorbance data is plotted as a function of wavenumber between 750 cm^{-1} and 3250 cm^{-1}. Some of the data is plotted on the graph and to clearly demonstrate the results, the vertical axis is made arbitrary. To understand the changes, the heights of the peaks are compared. The heights, in this case, are not measured from the bottom of the graph. Instead, they are measured from the beginning of the peaks to the top of them. Moreover, no plasma data is the same for all. Then, the changes are expressed considering corresponding peaks of no plasma data. Plasma species can only interact with the material surface; that is, first a few atomic layers are modified by the plasma [17]. How Ar plasma modifies chemical structures of PP surface are shown in Figure 4.1. The heights of peaks increase at 150 W, 200 W and 400 W. At 450 W and 500 W, there are two peaks decreased between 1210 cm^{-1} and 1260 cm^{-1} and these peaks refer to C-O vibrations[18].

How N_2 plasma modifies chemical structures of PP surface are shown in Figure 4.2. The height of the peaks at a specific wavenumber is proportional to the density of chemical band structures. Unlike Ar plasma treatment, the heights of peaks are increased up to 300 W. Then, peak intensities are lower than the untreated one. To compare Ar and N_2 plasma results at the same RF power, Figure 4.3 is plotted. On the one hand, the peak intensities due to N_2 plasma are almost always higher than Ar

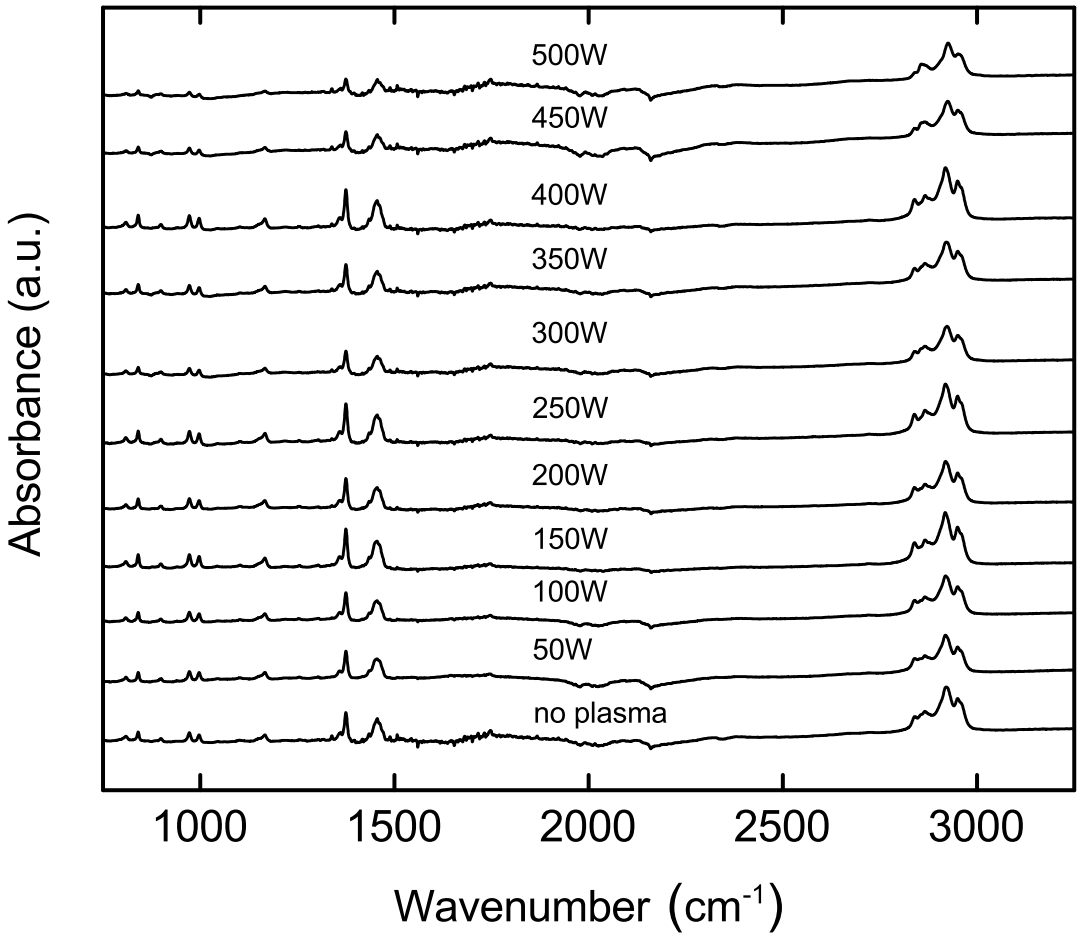

Figure 4.1: ATR spectra of PP modified by Ar plasma

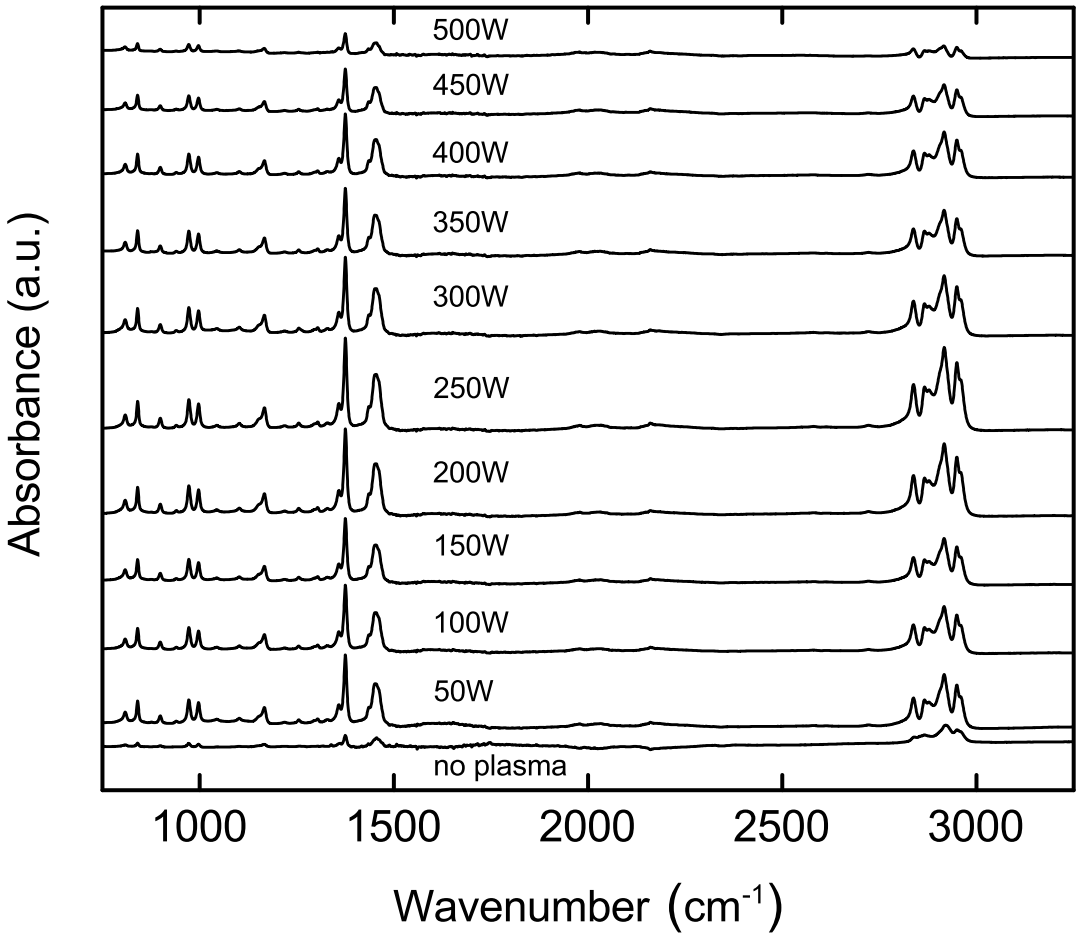

Figure 4.2: ATR spectra of PP modified by N_2 plasma

plasma. This implies there are more newly created structures in N_2 plasma. On the other hand, the N_2 plasma peaks between 2800 cm^{-1} and 3000 cm^{-1} have less height, shown in Figure 4.3j. These peaks are observed due to CH_x vibrations[17].

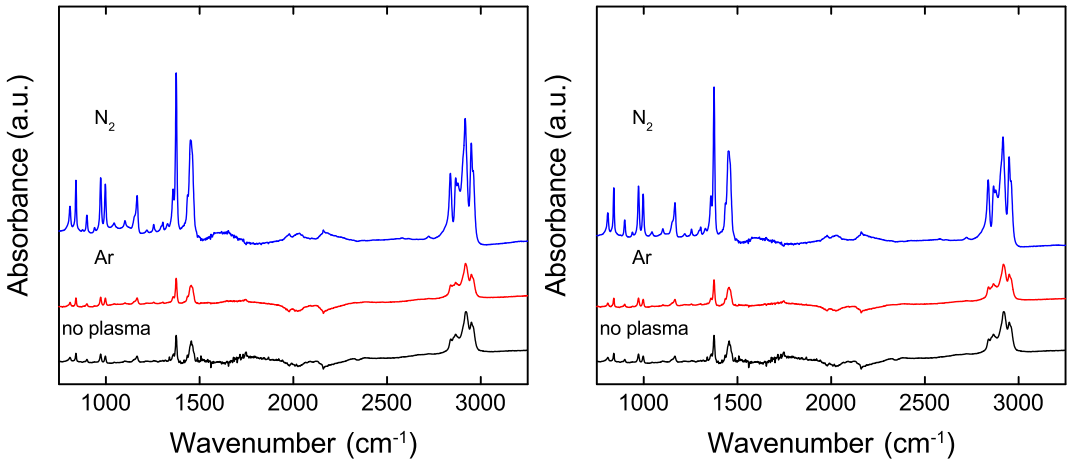

(a) 50 W

(b) 100 W

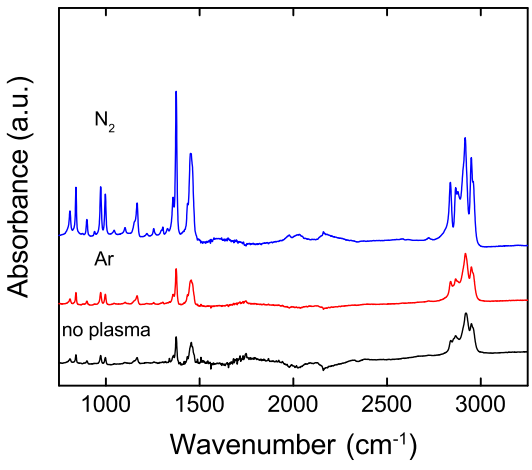

(c) 150 W

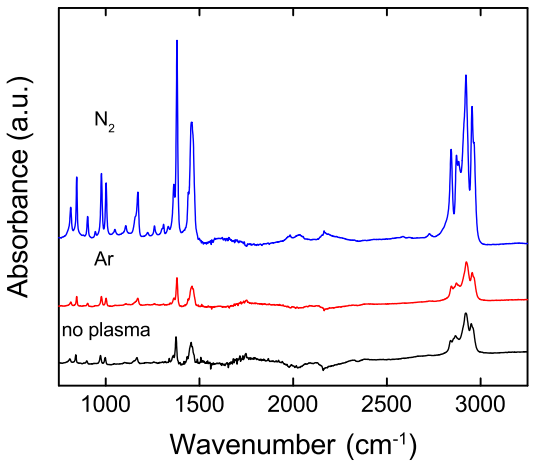

(d) 200 W

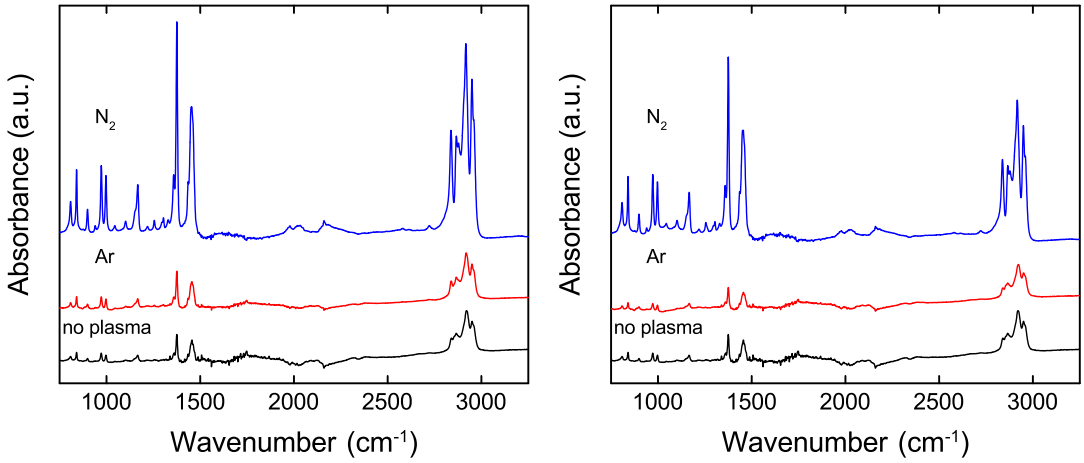

(e) 250 W

(f) 300 W

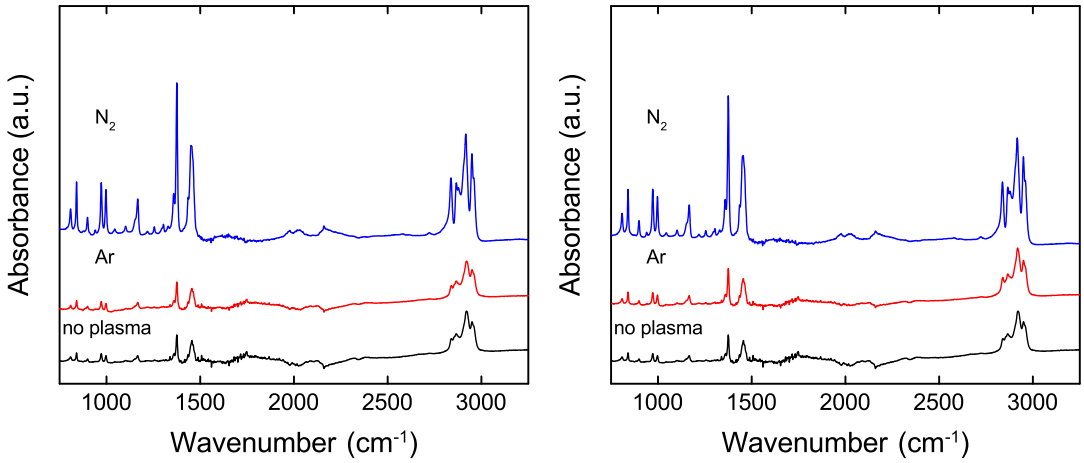

(g) 350 W

(h) 400 W

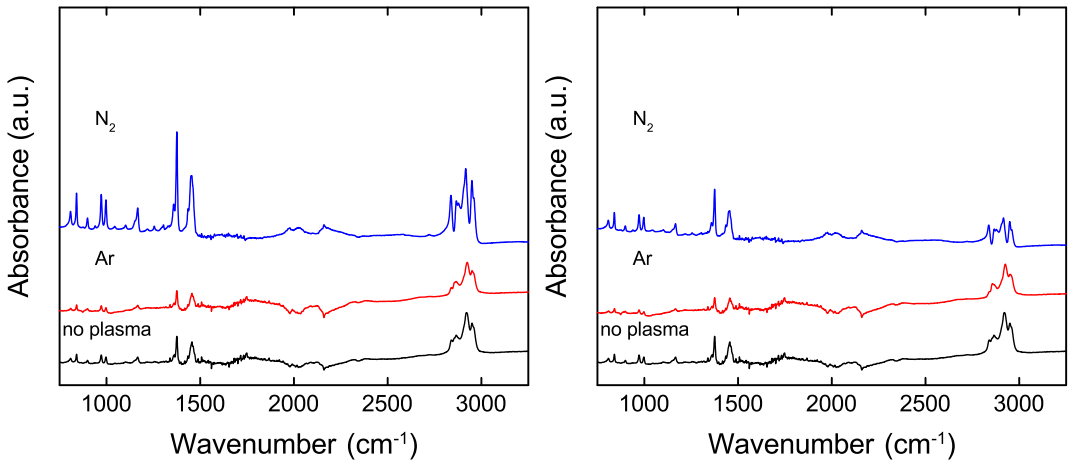

(i) 450 W

(j) 500 W

Figure 4.3: ATR spectra of the treatment at different RF powers

4.2 X-Ray Diffraction

The aim of these measurements is to observe the change in crystallinity of the PP, and it mainly has three crystalline phases, namely α-from, β-form and γ-form. Peaks are detected at 13.5°, 16.3°, 18.0°, 20.5°, 21.2°, 24.8°and 27.8°, shown in Figure 4.4 and 4.5. These point out α-form crystals with (110), (040), (130), (111), (131), (060), and (220) planes, respectively[19]. These figures show that the surface of modified PPs has more α-form crystalline type. The results also demonstrate not only crystalline regions but also amorphous ones. It could be seen that plasma-treated ones have fewer amorphous regions than the untreated one.

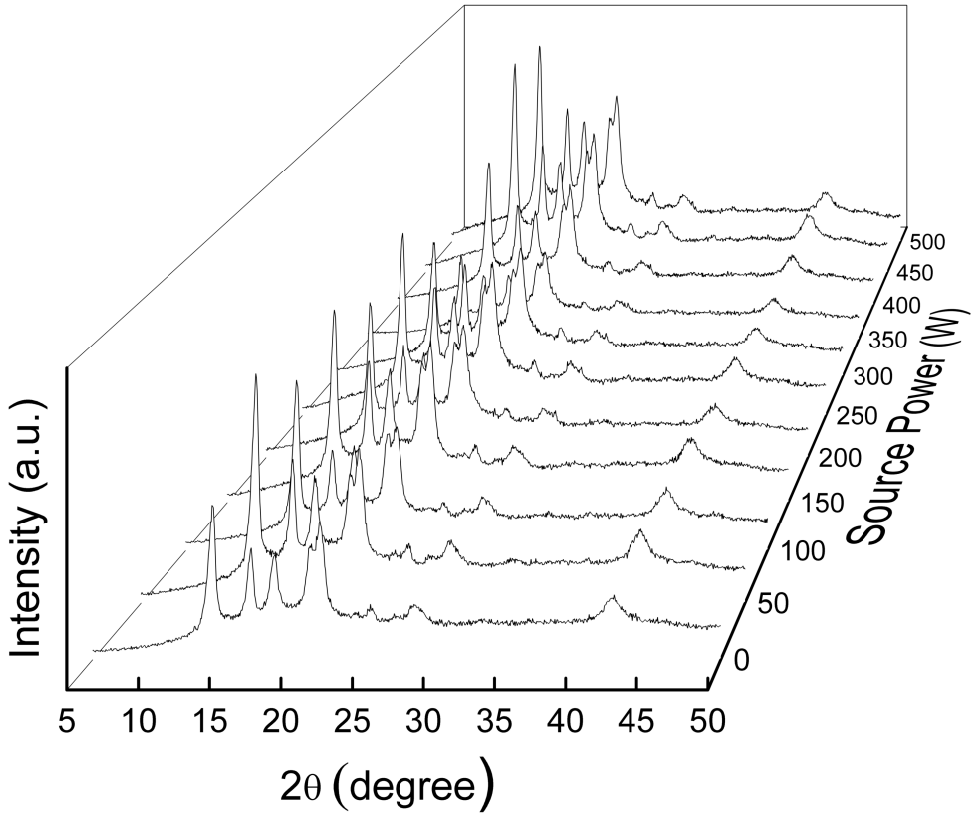

Figure 4.4: XRD Measurement of PP modified by Ar plasma

There is no always increase or decrease trend of the intensity in any case. N_2 plasma treatment cause sharper and high intensity peaks than Ar plasma and this implies more crystalline structures are obtained using N_2 plasma.

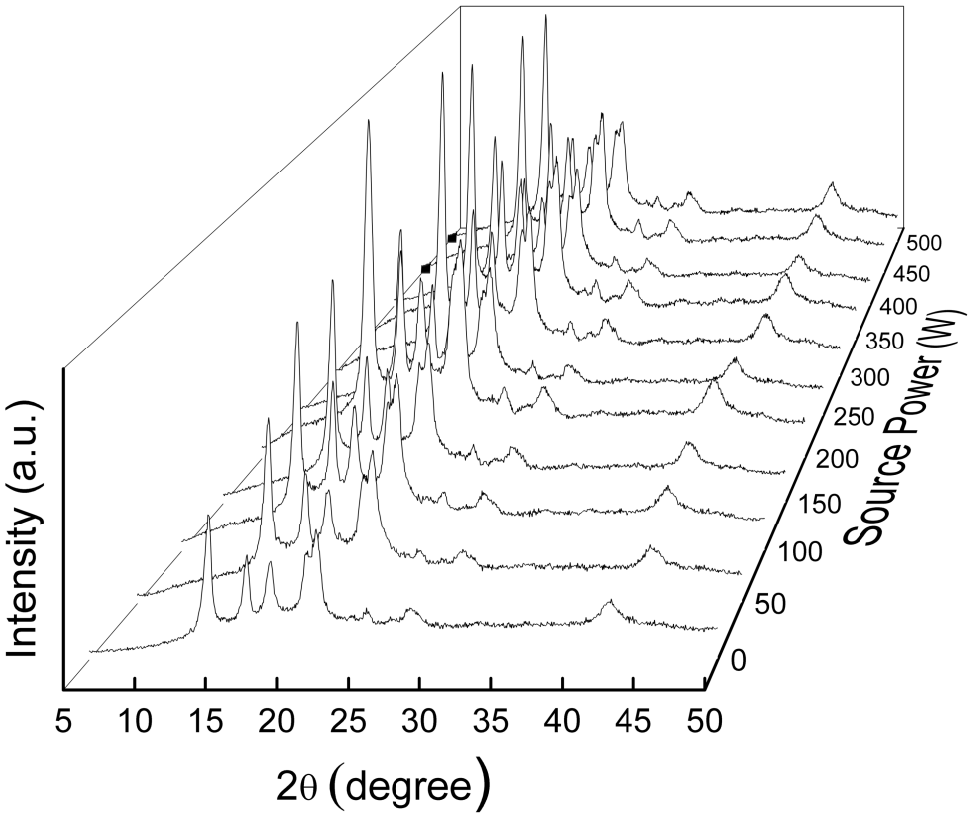

Figure 4.5: XRD Measurement of PP modified by N_2 plasma

4.3 Scanning Electron Microscopy

The aim of these measurements is to observe the change in surface morphology of the treated PPs. The untreated one has roughly a flat surface, shown in Figure 4.6. SEM images are taken with 50,000 times magnification. Ar plasma treatment leads great changes on the surface of PP. Due to Ar plasma at 150 W, irregular shapes formed on the surface, shown in Figure 4.7e. Increasing RF power to 250 W, more smooth structures are obtained, shown in Figure 4.7i. At 300 W, smaller(compared to treatment at 250 W) and regular shapes obtained as a result of Ar plasma treatment, as shown in Figure 4.7k. Also, higher RF powers cause large caves and bumps, shown in Figure 4.7q 4.7s. This could be because a layer is produced by Ar plasma treatment[20].

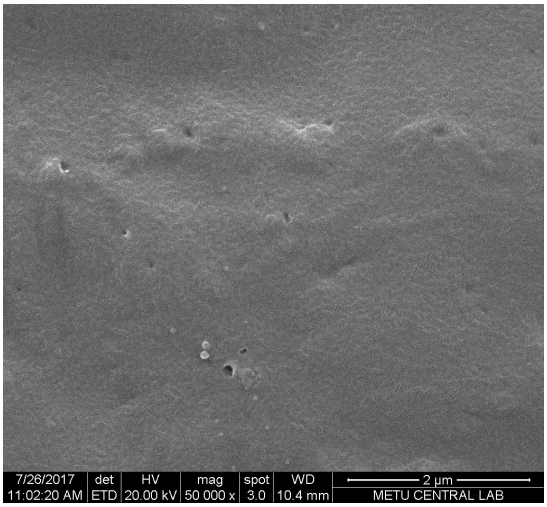

Figure 4.6: SEM image of PP

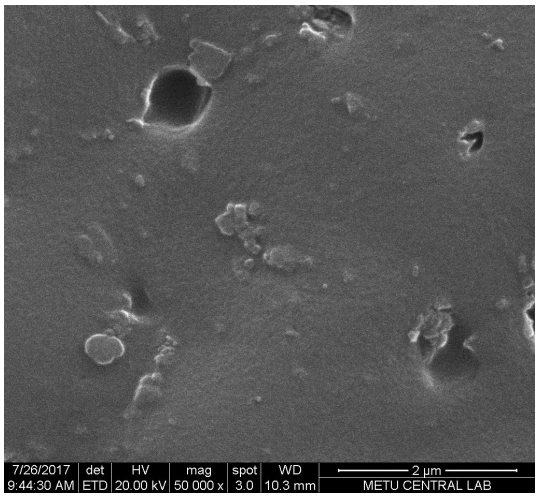

(a) Ar plasma at 50 W

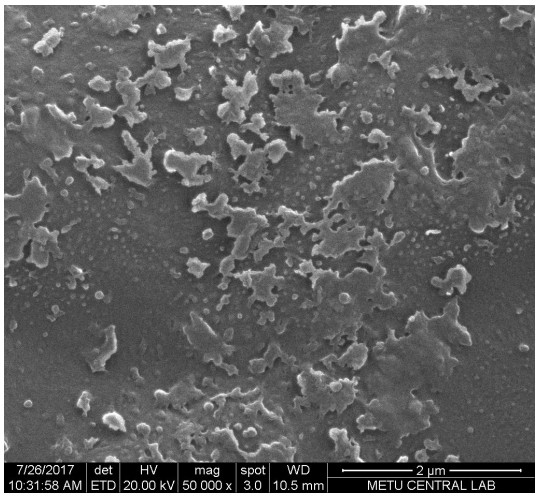

(b) N_2 plasma at 50 W

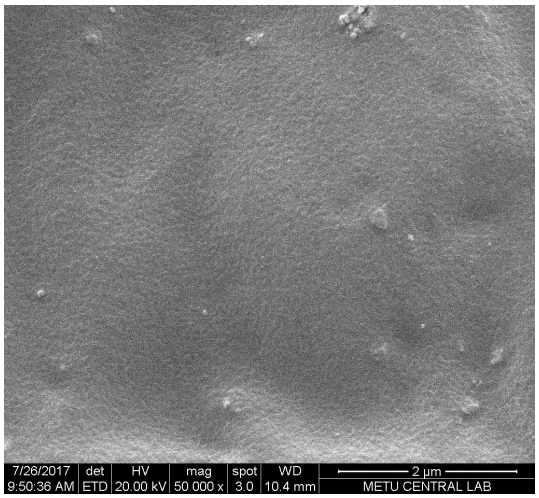

(c) Ar plasma at 100 W

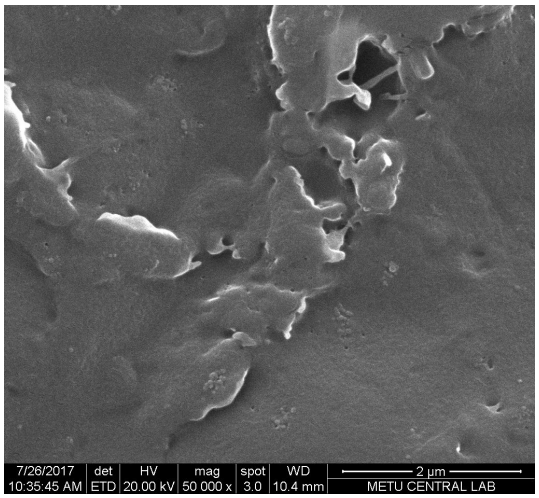

(d) N_2 plasma at 100 W

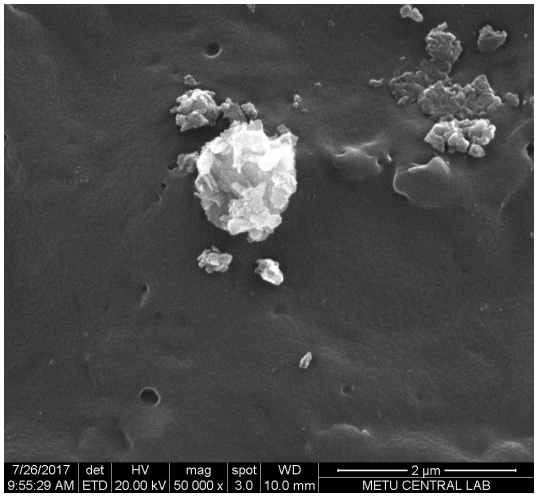

(e) Ar plasma at 150 W

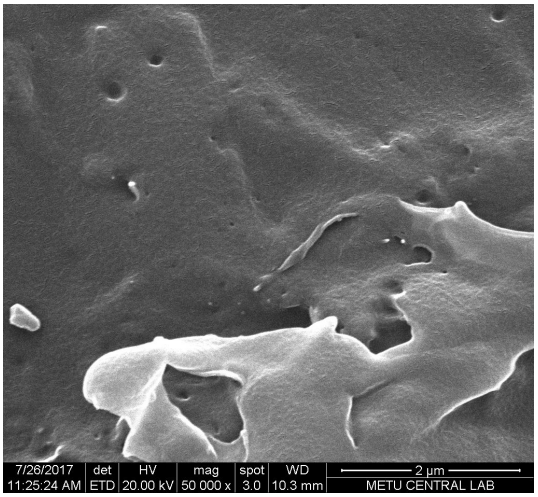

(f) N_2 plasma at 150 W

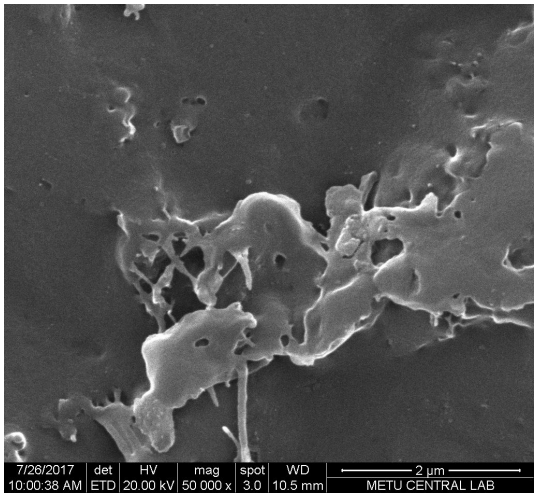

(g) Ar plasma at 200 W

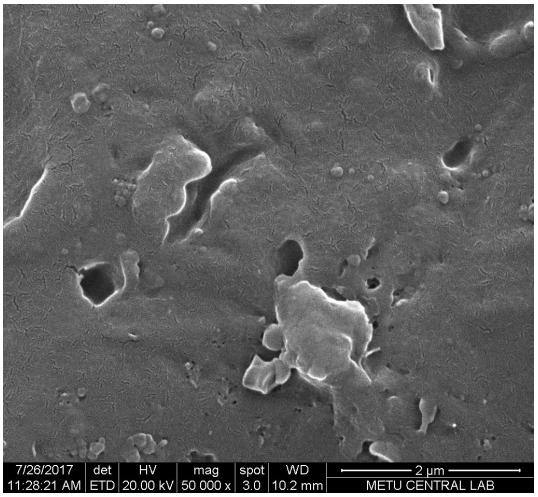

(h) N_2 plasma at 200 W

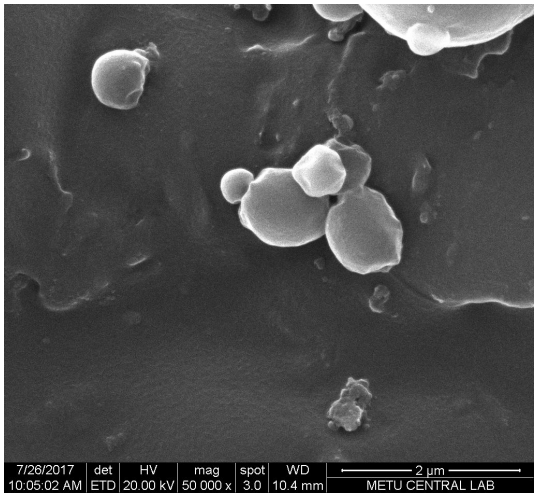

(i) Ar plasma at 250 W

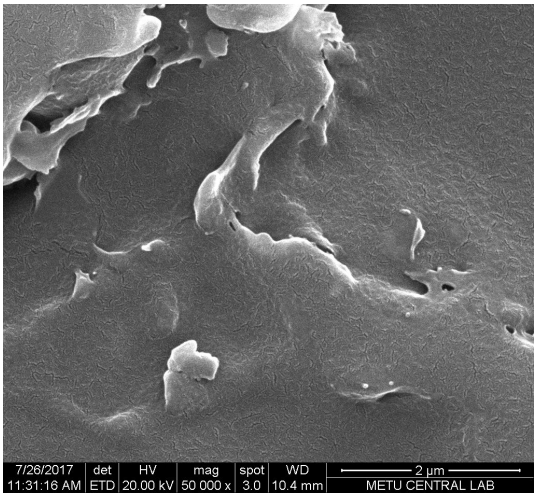

(j) N_2 plasma at 250 W

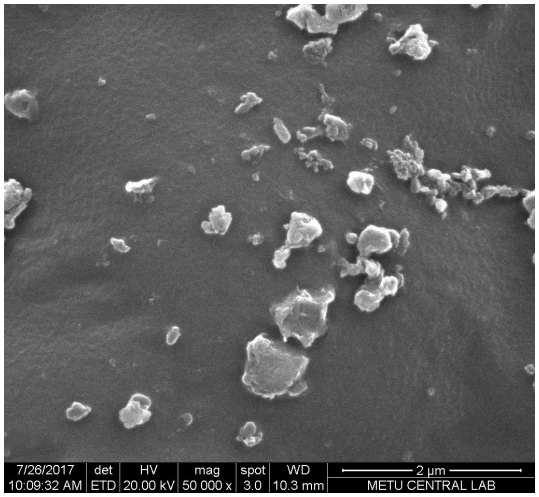

(k) Ar plasma at 300 W

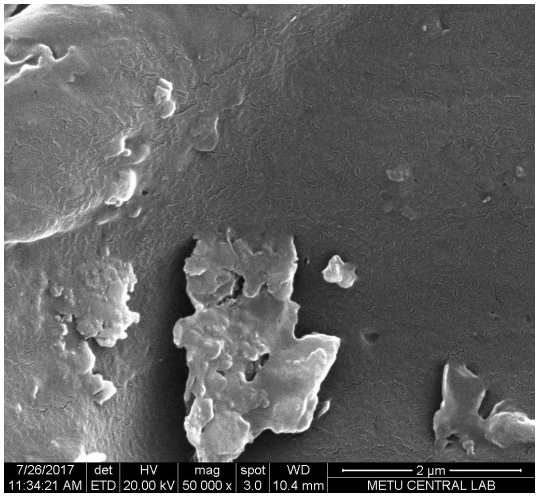

(l) N_2 plasma at 300 W

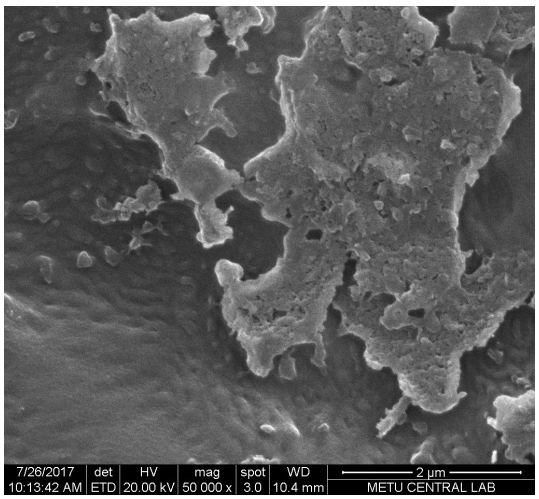

(m) Ar plasma at 350 W

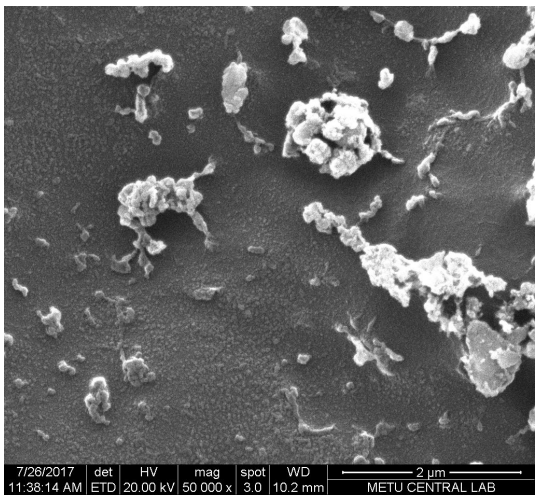

(n) N_2 plasma at 350 W

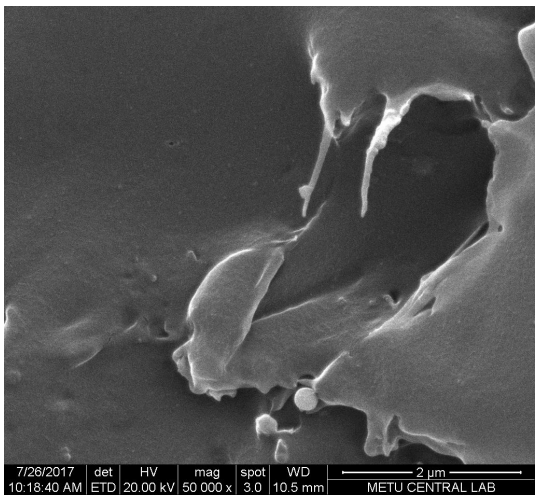

(o) Ar plasma at 400 W

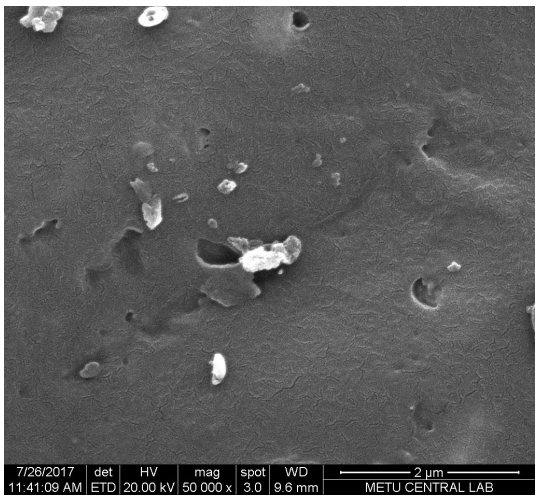

(p) N_2 plasma at 400 W

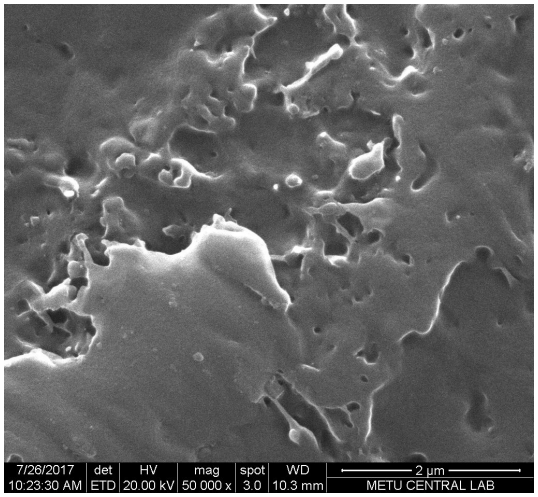

(q) Ar plasma at 450 W

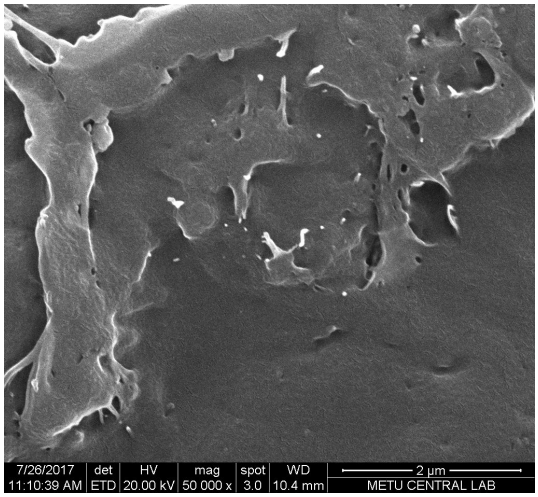

(r) N_2 plasma at 450 W

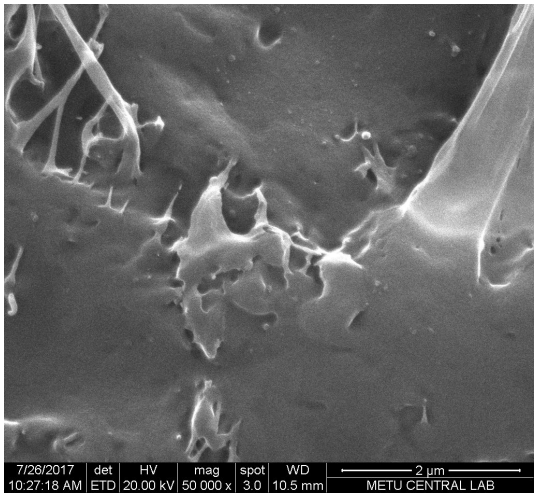

(s) Ar plasma at 500 W

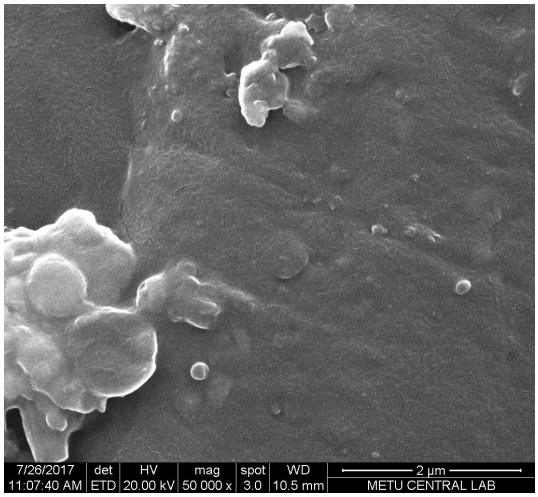

(t) N_2 plasma at 500 W

Figure 4.7: SEM images of treated PPs

N_2 plasma treatment results also give similar structures to Ar plasma but at different RF powers. As an example, N_2 plasma treatment result at 350 W has more irregular shapes, shown in Figure 4.7n, than as of Ar plasma treatment. These irregular shapes of N_2 plasma treatment are not grouped, instead of distributed around. In Figure 4.7t, there are two layers with different heights.

CHAPTER 5

CONCLUSION

In this thesis, PP samples are produced using PP beads. These samples are produced so that they are in suitable size with the analysis devices. PP surfaces are treated by a capacitively coupled RF plasma discharge system. This system is in vacuum and the pressure is kept constant for all treatments at 1.2×10^{-1} torr. A 13.56 MHz RF generator is used with its matching unit. Power range for the RF generator is 50 W to 500 W. Ar and N_2 gases at 50 sccm flow rate are utilized to create gas discharges for the treatment of the sample surfaces. Twenty different PP samples are treated. Physical and chemical changes are occurred and are observed in result of these treatments. All changes are compared with the untreated PP sample.

Using the ATR technique, chemical structures of treated and untreated PP samples are investigated. Up to 400 W, Ar plasma treatment results show increase of newly formed structures on the surface of the materials. After that, heights of the peaks decrease, so the density of the chemical bonds decrease. In other words, 450 W and 500 W treatments removes structures on the PP sample surface. For Ar plasma case, 400 W and 250 W treatments give the best results. However, all N_2 treatments have higher peak heights than Ar treatments. Most effective N_2 treatments are done at 250 W and 300 W.

ATR results are supported by XRD result. On the XRD figures, broaden peaks show amorphous structure, and sharp peaks show ordered structures. Plasma treatments make some broaden peaks sharper; hence, plasma treatments improve the crystallinity of PP samples. The improvement of crystallinity of PP samples increases with increasing RF power but there are some fluctuations. Considering crystallite size calculations published in [21], Ar treatment at 300 W shows higher crystallite size.

On SEM images, newly formed structures are observed. More regular and ordered

structures point out improved surface properties. Also, there are some caves on higher RF power images, and these observations are in harmony with ATR and XRD measurements. The results of N_2 plasma case is similar to as of Ar plasma, and indeed N_2 always modify more than Ar plasma.

In addition to these results, the wettability properties are examined and published in [22]. Contact angle measurements for all samples are done, and all treatments result in lower contact angle values. This shows hydrophilic surfaces are achieved. The best results are obtained Ar treatment at 350 W and N_2 at 50 W.

In conclusion, surface properties of PP samples are improved. On the RF power scanning range, some of treatments result in worsen or equivalent to untreated PP characteristics. Relatively good improvements are done in between 50 W and 350 W treatments. To deeply understand the relation between the plasmas and PP surface, further studies, that are not only examining power range but also exposure time, are needed.

REFERENCES

[1] J. M. Grace and L. J. Gerenser, "Plasma treatment of polymers," *Journal of Dispersion Science and Technology*, vol. 24, no. 3-4, pp. 305–341, 2003.

[2] L. Carrino, G. Moroni, and W. Polini, "Cold plasma treatment of polypropylene surface: a study on wettability and adhesion," *Journal of Materials Processing Technology*, vol. 121, no. 2, pp. 373–382, 2002.

[3] F. Awaja, M. Gilbert, G. Kelly, B. Fox, and P. J. Pigram, "Adhesion of polymers," *Progress in Polymer Science*, vol. 34, no. 9, pp. 948–968, 2009.

[4] E. Liston, L. Martinu, and M. Wertheimer, "Plasma surface modification of polymers for improved adhesion: a critical review," *Journal of Adhesion Science and Technology*, vol. 7, no. 10, pp. 1091–1127, 1993.

[5] D. A. Gurnett and A. Bhattacharjee, *Introduction to plasma physics : with space and laboratory applications.* Cambridge University Press, 2005.

[6] V. Krishan, *Plasmas : the first state of matter.* Cambridge University Press, 2014.

[7] F. F. Chen and J. P. Chang, *Lecture notes on principles of plasma processing.* Kluwer Academic/Plenum Publishers, 2003.

[8] L. Michael A. and L. Alan J., *Principles of Plasma Discharges and Materials Processing.*, vol. 2nd ed. Wiley-Interscience, 2005.

[9] U. S. Inan and M. Gołkowski, *Principles of Plasma Physics for Engineers and Scientists.* Cambridge University Press, 2011.

[10] R. Winkler, "The boltzmann equation and transport coefficients of electrons in weakly ionized plasmas," *Advances in Atomic Molecular and Optical Physics*, vol. 43, pp. 19–77, 2000.

[11] N. Inagaki, *Plasma surface modification and plasma polymerization.* Technomic Pub. Co., 1996.

[12] T. A. P. Hai, H. Matsukuma, and R. Sugimoto, "Surface modification of polypropylene with poly(3-hexylthiophene) via oxidative polymerization.," *Reactive and Functional Polymers*, vol. 122, pp. 167 – 174, 2018.

[13] G. Peter R. and H. James A. De, *Fourier Transform Infrared Spectrometry.*, vol. 2nd ed of *Chemical Analysis*. Wiley-Interscience, 2007.

[14] C. Kittel, *Introduction to solid state physics.* Wiley, 2005.

[15] J. Pouget, M. Jozefowicz, A. e. a. Epstein, X. Tang, and A. MacDiarmid, "X-ray structure of polyaniline," *Macromolecules*, vol. 24, no. 3, pp. 779–789, 1991.

[16] L. Reimer, *Scanning electron microscopy : physics of image formation and microanalysis.* Springer series in optical sciences: v. 45, Springer, 1998.

[17] J. Grace and L. Gerenser, "Plasma treatment of polymers.," *Journal of Dispersion Science Technology*, vol. 24, no. 3/4, pp. 305 – 341, 2003.

[18] E. Pretsch, P. Bühlmann, and C. Affolter, *Structure determination of organic compounds : tables of spectral data.* Springer, 2000.

[19] G. Machado, E. Denardin, E. Kinast, M. Gonçalves, M. de Luca, S. Teixeira, and D. Samios, "Crystalline properties and morphological changes in plastically deformed isotatic polypropylene evaluated by x-ray diffraction and transmission electron microscopy.," *European Polymer Journal*, vol. 41, no. 1, pp. 129 – 138, 2005.

[20] J. M. Warren, R. R. Mather, A. Neville, and D. Robson, "Gas plasma treatments of polypropylene tape.," *Journal of Materials Science*, vol. 40, no. 20, pp. 5373 – 5379, 2005.

[21] D. Mansuroglu, G. Mecit, and I. Umit Uzun-Kaymak, "A study of crystallization in plasma modified polypropylene.," *Materials Today: Proceedings*, vol. 18, no. Part 5, pp. 1964 – 1971, 2019.

[22] D. Mansuroglu and I. U. Uzun-Kaymak, “Argon and nitrogen plasma modified polypropylene: Surface characterization along with the optical emission results.,” *Surface Coatings Technology*, vol. 358, pp. 551 – 559, 2019.